Journal of High Energy Physics, Gravitation and Cosmology, 2026, 12(3), 1822-1834
https://www.scirp.org/journal/jhepgc
ISSN Online: 2380-4335
ISSN Print: 2380-4327

The Formation of Stars and Galaxies

Mark Linick

Independent Researcher, Long Beach, CA, USA
Email: marklinick@mindspring.com

How to cite this paper: Linick, M. (2026) The Formation of Stars and Galaxies. *Journal of High Energy Physics, Gravitation and Cosmology*, **12**, 1822-1834.
https://doi.org/10.4236/jhepgc.2026.123093

Received: May 7, 2026
Accepted: July 26, 2026
Published: July 29, 2026

Abstract

A novel pathway to star formation is explored based on condensation. We propose hydrogen clouds condense, producing degenerate condensates up to possibly galactic scale. For stellar-mass objects, accretion terminates once the parent cloud is exhausted. The surrounding envelope now produces heat from compression (Kelvin-Helmholtz), while degenerate electrons transfer heat to the core, lifting degeneracy. The gas is now thermally supported, producing the star. We then propose condensates of galactic mass may become unstable to collapse by neutronization and the removal of charge. The collapse can generate a rotation, followed by an explosion. Expelled material near the plane can contribute to disk formation, while expelled material near the spin axis may fall back, producing a smaller central condensate. This process cycles until the central component depletes, suggesting an outside-in disc development. Two totally different objects with unique developmental pathways, both start as a degenerate condensate. Together, these processes suggest a coherent, physically motivated framework linking condensation with unique structural formations across a wide range of astrophysical scales.

Keywords

Star Formation, Galaxy Formation, Degenerate Condensate, Hydrogen Cloud Condensation, Neutronization, Disk Formation

1. Introduction

Formation of stars and galaxies have always been associated with giant molecular clouds. The problem, then, is finding the mechanism that places the molecules into a smaller volume. Condensation is a novel, maybe overlooked, mechanism that seems to accomplish this function.

In standard stellar theory, gravitational collapse compresses gas until fusion ignites in the core [1] [2]. While physically consistent, this pathway relies on processes that differ from condensation. But a gas subjected to cooling typically condenses into a liquid or solid. It is therefore natural to ask whether condensation might also play a role in astrophysical processes.

Here, condensation is assumed, and explored as a product of a collapsing cloud. Through accretion, the condensate soon becomes degenerate. This form, the main topic of this argument, is believed to have the potential to become a star, and possibly other astrophysical objects.

When the accretion stops, presumably in some main sequence mass range, we examine the transformation of the condensate to a thermally supported gas, or a star. If the condensate accretes to some maximum mass, we examine the collapse to a larger mass object, presumably a galaxy.

Many existing models of star formation emphasize fragmentation and early dynamical collapse, often described through Jeans-type criteria [3]. These approaches favor the rapid breakup of clouds into smaller structures, which may limit the role of condensation. In the present work, we temporarily set aside fragmentation pathways in order to investigate whether a condensation route can provide an alternative or complementary perspective on the formation of stars and galaxies.

2. Condensation

We begin with a giant molecular cloud of hydrogen. We assume the cloud is isothermal and in hydrostatic equilibrium, radiating freely into space. What becomes of the cloud?

In contrast to Jeans-fragmentation, we offer the possibility that a cold gas will condense. The low temperature range needed for condensation (14 - 33 K) is readily achievable. Gravity dictates the direction of compression and the density profile. Both density and pressure are treated as an ideal gas. As compression continues, a liquid is inevitable in the temperature range.

Condensation begins at the radius where the ideal gas pressure first matches the saturation vapor pressure. Particles form droplets through adhesion in the vapor. Gravity then defines the direction of the condensate, causing droplets to fall inward and accumulate into a central liquid core. The vapor forms an atmosphere around the core.

When condensation starts, the gas and liquid are in equilibrium. The temperature of the liquid is set by the phase boundary, not by kinetics. The surface of the liquid has a temperature (~30 K, say) because that was the temperature of the cloud when it started to condense.

3. Structure of Condensate

As the mass increases, the condensate forms a layered structure dictated by pressure, shown in **Figure 1** below. Assuming a uniform density and the equation for pressure, Equation (1), we can estimate the maximum mass for the liquid/solid layers.

$$P_c = \frac{3GM^2}{8\pi R^4} \tag{1}$$

- **Liquid H_2 Layer**: From ~10^4 - 10^5 Pa to the surface (~20 - 30 K, density ~0.07 - 0.2 g/cm^3), this layer forms as low-pressure H_2 condenses [4] [5]. The maximum mass of the liquid shell is ~2.5×10^{17} Kg.
- **Solid H_2 Shell**: Extends from ~400 - 500 GPa (inner boundary, density ~0.7 - 1.5 g/cm^3) to ~10^4 - 10^5 Pa, where it transitions to liquid [6]. The shell accretes externally via continuous condensation. The maximum mass of the solid shell is ~9.0×10^{26} Kg.
- **Core**: At central pressures of 400 - 500 GPa, H_2 molecules dissociate and ionize due to pressure ionization, forming a dense, degenerate fluid (density ~1 - 2 g/cm^3) [7] [8]. The core grows as the inner surface of the solid H_2 shell evaporates, maintaining a steady-state pressure and density at the interface.

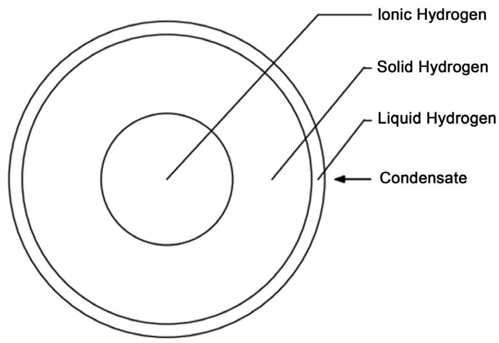

Figure 1. Structured layers of the condensate.

4. Evaporation

As the core grows, it becomes capable of evaporating the outer shells. We can estimate this core mass with a few assumptions.

For hydrogen, the heat of fusion, $L_{\text{fusion}} = 116$ kJ/kg, and the heat of vaporization, $L_{\text{vap}} = 446$ kJ/kg, for a total heat, $L = 562$ kJ/kg. Assume the total mas of hydrogen is the solid shell, $M = \sim 9.0 \times 10^{26}$ kg. Then the total energy needed to evaporate the shell is $L \times M$, or $E_{\text{heat}} = \sim 5 \times 10^{32}$ kJ.

Then assuming the core has a constant density of 1000 kg/m^3, we find the minimum mass of the core required to evaporate the shells from Equation (2), or $M = 1.4 \times 10^{25}$ kg, - about twice the mass of the Earth.

$$E_{\text{grav}} = \frac{3GM^2}{5R} = E_{\text{heat}} \tag{2}$$

Whether the shells fully evaporate or are assimilated does not influence the evolution. The point is a boundary exists, defined by the mass of the core. For lower mass degenerate cores, the shells survive and the object suggests a planet-like pathway. For higher mass degenerate cores, either the shell evaporates, or is progressively thinned and assimilated. Beyond this point, the core grows directly by cold gas accretion, and the object follows a stellar pathway.

After the shells evaporate, an ionic, non-degenerate gaseous layer forms above the core (the envelope). Its purpose is to absorb, then radiate, the heat from accretion. Once the cloud exhausts, its function is to heat the core. This enables a lower mass to become a star, or a larger mass to explode.

5. Accretion

With the outer layers dispersed or evaporated, the remainder of the cloud accretes as a cold gas onto the core. We assume in the absence of a typical luminous gas core, radial infall can continue to radiate away its energy efficiently, so that the degenerate core grows by cold accretion up to very large mass. This is analogous to Bondi accretion, but applied to a finite, collapsing cloud rather than a point mass in an infinite medium [9] [10].

We suggest accretion disks and polar jets, assumed mechanisms associated with accretion, are post stellar products, made visible once the star becomes luminous [11] [12].

6. Support of Condensate

Similar to stars, pre-stellar condensates are supported by charge. This is a consequence of the behavior of Fermi electrons. Since this behavior deviates from current theory, a brief explanation is provided before considering examples. The explanation is similar to the behavior leading to supernovas [13].

In current theory, electron degeneracy pressure supports the mass of a star. In this theory, it does not. Degeneracy pressure cause the electrons to expand through the mass. This separates the charge. It's the positive charge that supports the mass (itself), not the electrons.

In supernovas, a core collapse cause electrons to expand relative to the falling ions. This rapidly separates the charge, enough to cause an explosion. But most of the life of a star is spent in a type of steady state. Moderate density increases allow the protons to follow the expanding electrons (like charges repel). Gravity prevents them from ever catching up. This is similar in our condensate, where charge always supports the mass to some degree, but at a much lower temperature.

Further, the Chandrasekar limit is not considered. You can use the fermi electron pressure in the equation of hydrostatic equilibrium to get a density profile, because the protons end up following the electrons. But you can't use it to calculate the mass—it cancels out the density in the equation for mass. This gives you a constant, and incorrect, mass—the Chandrasekar limit.

To find the charge, divide the condensate (or star) into shells. Assume the ions stationary. The change in Fermi pressure in the current shell will displace electrons radially. Electrons collecting at the Fermi radius, R_f (the radius at ~10^6 kg/m^3), seems reasonable, assuming all available states inside this radius are occupied. This creates a coulomb pressure, with N, the number of charges displaced and A_f, the area at the fermi radius:

$$P_q = K\left(N/A_f\right)^2 \tag{3}$$

where $K = 12\pi K_q\left(q^2\right)/5$ and $K_q \sim 9\times10^9$. We can model this distribution, solve for N (N_- or N_+), by equating the difference in Fermi pressures caused by the displaced electrons, or $\Delta P_F = P_q$. The Fermi pressure in the current shell, P_F, changes with number density as the electrons expand as follows:

$$\begin{aligned}\Delta P_F &= (hc/4)(3/8\pi)^{1/3}\, n_\Delta^{4/3} \\ &= K_F\left((N_F - N)/V_F\right)^{4/3} \\ &= P_F(1 - N/N_F)^{4/3} \\ &= P_F\left(1 - (4/3)N/N_F\right) \quad (1^{\text{st}}\ \text{order}) \\ &= P_F - (4P_F/3N_F)N\end{aligned}$$

Then solving for *N*,

$$\left(K/A_f^2\right)N^2 + \left(4P_F/3N_F\right)N - P_F = 0 \tag{4}$$

Now model the mass using Lane-Emden and the following criteria:

- Density (degenerate-like profile, normalized to match the mass):

$$\rho(r) = \rho_c\left(1 - r^2/R^2\right)^{3/2}, \quad \rho_c = 2.0\times10^{10}\ \text{kg/m}^3$$

- Fermi radius (r_f) defined by $\rho(r_f) = 10^6\ \text{kg/m}^3$
- Divide into 1000 shells from 0 to r_f
- Cap charge due to neutronization:

$$\rho_{\text{charge}} = \min\left(\rho, 10^{10}\ \text{kg/m}^3\right)$$

- Relativistic degeneracy pressure (index 4/3):

$$P_F = K_{\text{rel}}\rho_{\text{charge}}^{4/3}$$

Now sum the charge in each shell and compare the coulomb to gravitational energies:

$$\left(K_q Q^2\right)/\left(GM^2\right) = \eta \tag{5}$$

For example, consider a 200 solar mass condensate, with a central density of 2 × 10^{10} kg/m^3. Then,

$$200M_\odot : \eta \sim 10^5 \tag{6}$$

This procedure calculates the maximum charge for each shell (each density). If the charge is greater than the gravitational mass ($\eta > 1$), the charge expands until it equals the gravitational mass ($\eta = 1$). This decreases the density and increases the volume of the condensate. This is the steady state described earlier. However, it appears the maximum charge calculated will easily support the mass of any star, up to $200M_\odot$.

7. End of Accretion

As long as the condensate accretes cold gas, the surrounding non-degenerate envelope remains optically thin and cannot trap radiation efficiently. Under these conditions, compressional heating is radiated away and the condensate remains cold and degenerate.

When the parent cloud exhausts, accretion effectively stops. The envelope becomes optically thick, trapping radiation in a greenhouse-like manner. Compressional heating proceeds on a Kelvin-Helmholtz timescale, causing the temperature of the envelope to rise.

This heating lifts degeneracy in the outer layers of the condensate and promotes the onset of fusion. Because degenerate electrons conduct heat efficiently, thermal energy is transported inward, heating the condensate from the outside in. This contrasts with standard stellar models, where the core heats the envelope from the inside out.

As the temperature rises, thermal pressure contributes to support, reducing the central density and lifting degeneracy. The condensate then transitions into a thermally supported, main-sequence configuration.

For main sequence condensates, charge increases the volume, making the condensate less dense. Lower densities are easier to expand thermally due to gravity. This would not be true for higher mass condensates (galactic), explained later.

If degeneracy cannot be lifted thermally within or above the main-sequence mass range, sufficiently high temperatures may induce pair production, softening the equation of state and potentially triggering collapse or explosive behavior. In the present work, however, we assume degeneracy can be lifted thermally for hydrogen condensates across the stellar main-sequence mass range.

8. Maximum Mass

It is plausible there is a maximum mass, with implications of galaxy formation. For galactic-scale condensates, central densities can approach ~10^{10} kg/m^3 once the mass reaches $\sim 10^{12} M_\odot$ (the mass of Hoag's object, discussed later). At these densities, neutronization begins to remove charge, limiting further growth of charge support.

Beyond this point, additional increases in density arise primarily from neutrons, while the effective charge support saturates near the ~10^{10} kg/m^3 limit. As a result, further mass growth increasingly favors gravity over additional charge support. As an example, consider a $\sim 10^{12} M_\odot$ condensate, with a central density of 2×10^{10} kg/m^3. Then,

$$\sim 10^{12} M_\odot : \eta \sim 0.1 \tag{7}$$

Compare Equation (7) with Equation (6). Gravity is now dominant over charge. We propose this leads to a feed-forward mechanism of charge removal, followed by the collapse and explosion of the condensate.

Already marginally unstable ($\gamma = 4/3$), once the condensate crosses this mass regime, three effects promote collapse: 1) progressive removal of charge via neutronization, 2) increasing pressure from the existing mass, and 3) continued mass growth from accretion. A small initial contraction increases the density further, accelerating neutronization and charge loss. Provided the rate of neutronization exceeds the rate at which the remaining charge can re-establish support, this feed-forward process leads to rapid collapse. The ensuing collapse separates the remaining charge, releasing sufficient energy to drive an explosion.

9. Angular Momentum

Most objects in the universe spin. And we have previously shown, most objects beginning as a condensate, collapse. We now want to show a correlation between the collapse of the condensate and the production of angular momentum. This includes the evolution of the condensate into a star, where the collapse precedes a supernova, and the collapse of a massive condensate, suggesting a galaxy.

Starting from negligible or zero initial fields (with little or no rotation), seed magnetic fields are generated (Biermann battery) during the initial phases of collapse and explosion [14]. The Weibel instability then amplifies these fields, converting kinetic energy into magnetic energy [15]. Charged particles (e.g., ions and electrons) falling through this amplified magnetic field can produce torque and spin.

To estimate the rotation, or the angular momentum (L), we consider the torque (τ) induced by the magnetic field on currents in the collapsing object, integrated over time. Angular momentum is given by $L = \int \tau \mathrm{d}t$, where $\tau = r \times F$, and F arises from the Lorentz force on induced currents.

Consider a $200M_{\odot}$ object of degenerate hydrogen condensate (or an ionized gas) with radius, $R_{\circ} \approx 8.4 \times 10^{8}\ \mathrm{m}$. Assume an amplified magnetic field, $B = 1$ mT (10^{-3} T) [16]. We demonstrate as follows:

9.1. Induced Currents

- During collapse, a changing flux induces an electromotive force (EMF): $\epsilon = -\mathrm{d}\Phi/\mathrm{d}t$, where $\Phi = B \cdot A$, and $A \sim \pi R^{2}$ is the cross-sectional area.
- For a collapsing sphere, the collapse time, $t_{c} \approx (G\rho)^{-\frac{1}{2}} \approx 10^{3}\ \mathrm{sec}$.
- $\mathrm{d}\Phi/\mathrm{d}t \sim B \cdot \mathrm{d}A/\mathrm{d}t$, where $\mathrm{d}A/\mathrm{d}t \sim 2\pi R \cdot \mathrm{d}R/\mathrm{d}t$. If $\mathrm{d}R/\mathrm{d}t \sim -R_{\circ}/t_{c}$, then $\mathrm{d}\Phi/\mathrm{d}t \sim B \cdot 2\pi R_{\circ} \cdot (-R_{\circ}/t_{c})$.

  Then, $\epsilon = -\mathrm{d}\Phi/\mathrm{d}t \approx -4.4 \times 10^{12}\ \mathrm{V}$.
- The induced current is $I \sim \epsilon/R_{e}$, where R_{e} is the electrical resistance. For metallic hydrogen, $\sigma \sim 10^{8}\ \mathrm{S/m}$ and $R_{e} \sim \ell/(\sigma A) \sim 2\pi R_{\circ}/(\sigma \pi R_{\circ}^{2}) \sim 2/(\sigma R_{\circ})$.

  Then, $I \sim \epsilon \cdot \sigma \cdot R_{\circ}/2 \approx 2.0 \times 10^{29}\ \mathrm{A}$.

9.2. Torque and Angular Momentum

- The torque, $\tau = r \times F$, where $F = I \cdot \ell \times B$ and $\ell = 2\pi R_{\circ}$.

  Then $\tau \sim I \cdot B \cdot R_{\circ}^{2} \approx 1.4 \times 10^{44}\ \mathrm{N \cdot m}$.
- The angular momentum, $L \sim \tau \cdot t_{c} \approx 1.4 \times 10^{47}\ \mathrm{kg \cdot m^{2}/s}$ if integrated over the full collapse.

This ideal calculation overestimates. Still, at 10 or 100 times less, this is a very large number.

Finally, an enigma (to some) seems to support this mechanism. The magnetic seed fields generated by the Biermann battery are amplified in directions that are determined by the local geometry of the collapsing object. There is no global influence. This explains why the spin axis of all objects in the universe point in different (random) directions.

10. The Formation Cycle

From the argument on Supernovas [13], only the core has sufficient density to explode, to separate the charge on collapse. The explosion propels the surrounding inert condensate (or gas) outward, but never to infinity. This material will recollapse.

Combined with the mechanisms of this argument, we have a process that repeats, over and over. Each condensate produced becomes progressively smaller after each explosion. One may guess a star or sun as the end product, but this view is too narrow. The process is cumulative and can form a galaxy. An array of objects are possible.

The process broadens the definition of solar system. An exploding, spinning sphere produces a spherical shell. The shell collapses along the spin axis, forming a smaller mass, and flattens in the equatorial plane, forming a disk.

A smaller mass exploding produces the traditional solar system (with planets). A larger mass exploding produces a disk with stars (a binary or trinary system). If the cloud is rotating, two collapsing masses in close proximity may orbit each other. A disk may form without condensations.

When the condensate reaches a maximum mass, a galaxy (or disc) may form. The initial explosion should define the rotation of all subsequent condensates. If each explosion produces smaller condensates, then each explosion should produce smaller rings, each ring just inside the previous. Then the disc should form from the outside in.

As the disc develops, mass and density increase as evidenced by an increasing gradient to the inside. Explosions now transfer mass and angular momentum directly to the face of the inner radius, until the central condensate exhausts.

The central core now appears empty (no black hole), in contrast to current theory. However, the premise is promising, and may provide an alternate theory for galaxies with further research.

Finally, this mechanism may explain more mysterious objects, such as ring galaxies (Hoag's object). These objects have a core of older, yellow stars, surrounded by a much younger ring. How is this object produced?

If the older core merges with a galactic cloud, the cloud may condense to the center and explode, producing the ring. There is also a remnant that falls back along the spin access. Since only one ring is produced, we assume this gas accretes onto the older stars. Perhaps some signature of this possibility can be detected.

11. Circular Velocity Profiles

We continue our discussion on galaxy formation by examining the development of the disc. In particular, the galactic disc exhibits a curious linear circular velocity profile. By examining this profile, together with assumptions concerning the initial cloud collapse, we can explain how this profile is produced. This explanation implies a continuous production of angular momentum from the core, consistent with the discussion in the previous section.

Velocity Profile Apparently, scientists are able to measure the circular velocity of stars in the discs of galaxies quite accurately. Of the many papers that plot these measurements, the one by Eilers *et al.* [17] was attractive because they plotted the Milky Way.

Figure 2(a) shows a declining linear profile of circular velocities in the disc of the Milky Way. As noted in their discussion, this is rare. Most galaxies have a flat or increasing circular velocity profile.

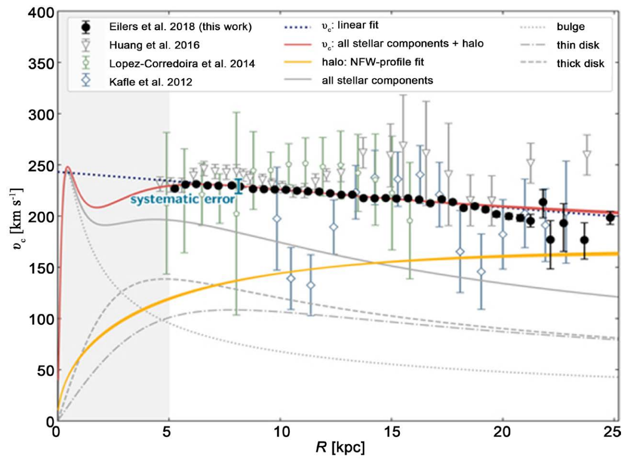

(a) Linear velocity profile in disk of Milky Way

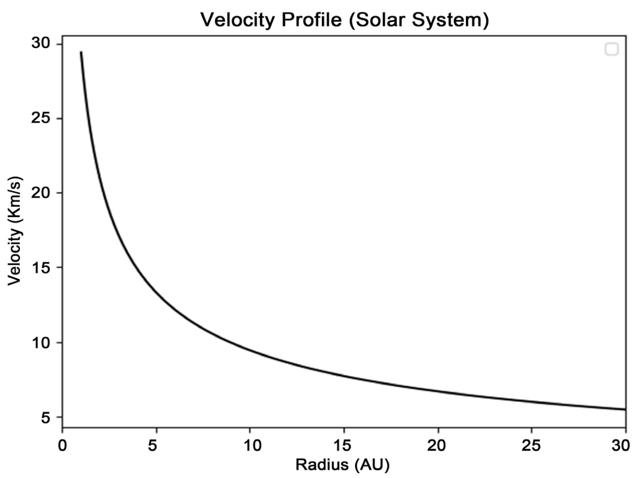

(b) Velocity profile $\propto r^{-\frac{1}{2}}$ in our solar system

Figure 2. Circular velocity profiles of (a) a galaxy and (b) a solar system.

As a comparison, a plot of orbital velocities in our solar system is shown in Figure 2(b). Despite the contrast, a difference should be expected. An object in the disc orbits the mass it sees inside, whereas objects in solar systems orbit the same central mass. However, the linear profile is mysterious and what we wish to examine.

In Figure 3(a), we plot an ideal linear circular velocity profile ($v = mr + b$) between the inner and outer radius for three cases: the outer radius velocity is less than, equal to or greater than the inner radius velocity. We then calculate the unique mass (2 types) and density profiles using an orbital equation for each velocity profile ($M = rv^2/G$), as shown in the Figures 3(b)-(d).

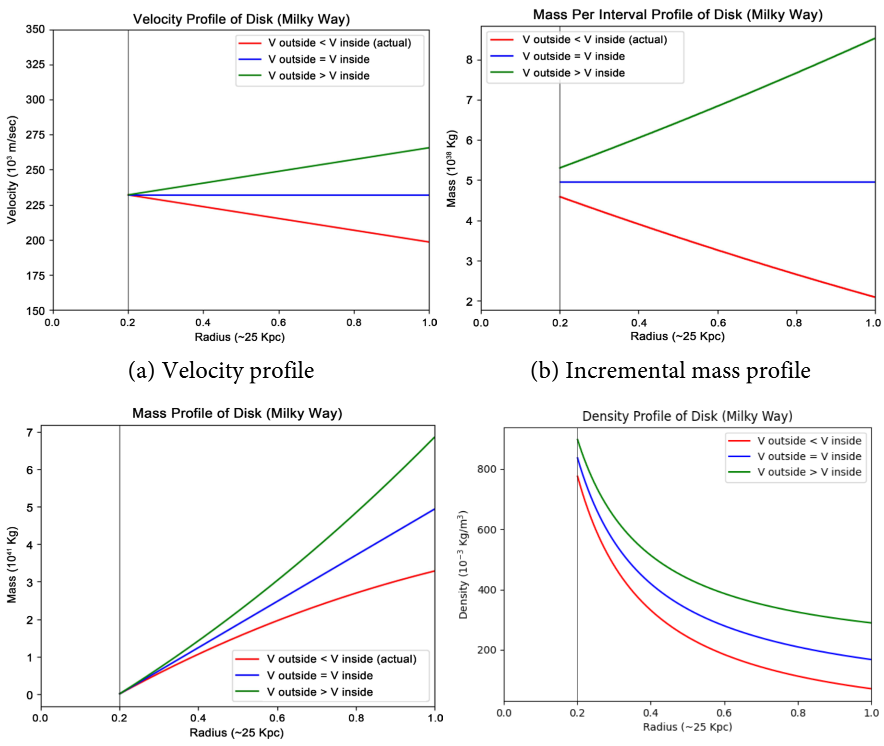

(a) Velocity profile (b) Incremental mass profile

(c) Total mass profile (d) Density profile

Figure 3. Profiles showing the velocity, incremental mass, total mass and density, where the outer radius velocity is less than, equal to or greater than the inner radius velocity.

Nothing stands out to explain the spectrum of profiles. However, the top profile in Figure 3(a) is similar to a rigid rotator. A rigid rotator produces an increasing linear velocity profile by definition, $v = r \cdot \omega$. This may make sense if the disc rotates as one piece at the beginning of development. Examining the density of the disc can shed more light.

Density Profile Assume the cloud forming the galaxy is close to isothermal, just before and during the collapse. Then pressure is proportional to density, and from the equation of hydro-static equilibrium, the density of the cloud is proportional to r^{-2}, or:

$$\rho = k/r^2 \tag{8}$$

As the cloud begins to spin, portions away from the center become static due to centrifugal force and fall vertically along the spin axis. This forms the disc in the central plane. Then using Equation (8), the disc will form with a density profile proportional to r^{-1}, or:

$$\rho = k/r \tag{9}$$

Equation (9) is the initial density of the disc. Since it contains the same mass in less space, it reduces the radius of the disk. We plot this profile (Equation (9)) together with the actual profile (Figure 3(d)) in Figure 4 below. It implies the initial disc of radius 19.4 Kpc migrated, producing the current disc of radius 25 Kpc. We discuss this migration next.

Disc Migration Recall we are interested in explaining the linear velocity profiles in galactic discs. If galactic discs begin as a rigid rotator, migration (if any) will help produce the final profile we seek.

The plots in Figure 4 imply the disc migrates as the galaxy develops. The disc begins to migrate when the rotational speed of the outer radius matches its orbital velocity. As the spin increases, layers inside the outer radius will nudge it into higher orbits through a viscous type of "gas friction". As the rotation increases, successive layers behave in a similar manner.

This mechanism causes the circular velocities of successive layers to be close and duplicate the patterns shown in Figure 2(a). This is not like planets orbiting a central mass. As a disc, each layer is orbiting the mass it sees inside and allows the profile to remain linear.

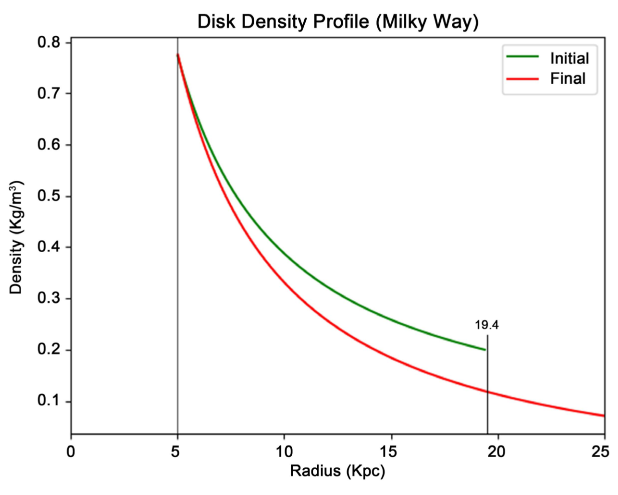

Figure 4. Initial vs final disk density profile of Milky Way. Both profiles contain the same amount of mass. The initial radius of the disc was 19.4 Kpc.

As the disc expands (migrates), the orbits of the outer layers become slower, rotating the circular linear velocity profile clockwise. This makes the profiles in Figure 3 more understandable, as each profile applies to a different disc size (before and after migration). The increasing velocity profile implies a rigid rotation;

the decreasing velocity profile implies an orbital rotation. There is no "dark matter" required for this mechanism.

The problem now is to find the source of angular momentum. There are popular theories where the initial cloud inherits angular momentum. A cloud possessing angular momentum will increase its rotation as it collapses. But the disc radius and its rate of rotation are the final products. This would not work with the mechanism described in this section. The disc needs to *increase* its rate of rotation *after* it forms to migrate. This implies a continuous central source of angular momentum, consistent with the "collapse and explode" mechanism described earlier.

12. Conclusions

It appears condensation can take place in a collapsing cloud under calm, isothermal conditions, offering an alternative to current stellar formation theory. Condensation places the gas in the smallest possible volume—a natural starting point for stellar formation. As the condensate grows, it becomes degenerate, accreting mass from a non-degenerate envelope surrounding the core.

The surrounding envelope radiates efficiently, keeping the condensate cool and growing. When accretion stops, the envelope heats through Kelvin-Helmholtz contraction. Degenerate electrons transfer the heat to the core, lifting degeneracy. The condensate becomes a thermally supported gas (a star). In this way, a main-sequence star can emerge from a cold, degenerate precursor, in contrast to standard inside-out heating scenarios.

In addition, the condensate can become unstable at a maximum galactic mass, as neutronization removes charge support. The ensuing collapse of the condensate at low temperature is analogous to a stellar collapse (supernova) at high temperature. Further, a collapse can naturally cause the degenerate condensate (or an ionized stellar gas) to rotate. The possibility of galaxy formation was described earlier.

This argument provides a coherent, plausible pathway for various astrophysical objects in the universe. Recalling the non-degenerate condensate may provide a platform for planets. While many aspects of this model require further development, the results suggest that condensation may play a fundamental role.

Conflicts of Interest

The author declares no conflicts of interest regarding the publication of this paper.

References

[1] Wikipedia Contributors (2024) Star Formation. Wikipedia, The Free Encyclopedia.

[2] Klessen, R.S. and Glover, S.C.O. (2023) The First Stars: Formation, Properties, and Impact. *Annual Review of Astronomy and Astrophysics*, **61**, 65-130. https://doi.org/10.1146/annurev-astro-071221-053453

[3] Jeans, J.H. (1902) I. the Stability of a Spherical Nebula. *Philosophical Transactions of the Royal Society of London*. *Series A*, *Containing Papers of a Mathematical or Physical Character*, **199**, 1-53. https://doi.org/10.1098/rsta.1902.0012

[4] Souers, P.C. (1986) Hydrogen Properties for Fusion Energy. University of California

Press.

[5] Dias, R. P. and Silvera, I. F. (2017) Observation of the Wigner-Huntington Transition to Metallic Hydrogen. *Science*, **355**, 715-718. https://doi.org/10.1126/science.aal1579

[6] Datchi, F., Loubeyre, P. and LeToullec, R. (2000). Extended and Accurate Determination of the Melting Curves of Argon, Helium, Ice (H_2O), and Hydrogen (H_2). *Physical Review B*, **61**, 6535-6546. https://doi.org/10.1103/PhysRevB.61.6535

[7] McMahon, J.M., Morales, M.A., Pierleoni, C. and Ceperley, D.M. (2012) The Properties of Hydrogen and Helium under Extreme Conditions. *Reviews of Modern Physics*, **84**, 1607-1653. https://doi.org/10.1103/revmodphys.84.1607

[8] Loubeyre, P., *et al.* (2020) Synchrotron Infrared Spectroscopic Evidence of the Probable Transition to Metal Hydrogen. *Nature*, **577**, 631-635. https://doi.org/10.1038/s41586-019-1927-3

[9] Smith, M.D. (2014) Evolutionary Tracks of Massive Stars during Formation. *Monthly Notices of the Royal Astronomical Society*, **438**, 1051-1066. https://doi.org/10.1093/mnras/stt2210

[10] Bhandare, A., Ali Ahmad, A. and Commerçon, B. (2025) Turn up the Light: Radiative Efficiency of Protostars at Birth. *Astronomy & Astrophysics*, **702**, L7. https://doi.org/10.1051/0004-6361/202556128

[11] Frank, J., King, A. and Raine, D. (2002) Accretion Power in Astrophysics. 3rd Edition, Cambridge University Press. https://doi.org/10.1017/cbo9781139164245

[12] Pudritz, R.E., Hardcastle, M.J. and Gabuzda, D.C. (2012) Magnetic Fields in Astrophysical Jets: From Launch to Termination. *Space Science Reviews*, **169**, 27-72. https://doi.org/10.1007/s11214-012-9895-z

[13] Linick, M. (2025) Supernovas. *Journal of High Energy Physics*, *Gravitation and Cosmology*, **11**, 275-283. https://doi.org/10.4236/jhepgc.2025.112023

[14] Schoeffler, K.M., Loureiro, N.F., Fonseca, R.A. and Silva, L.O. (2016) The Generation of Magnetic Fields by the Biermann Battery and the Interplay with the Weibel Instability. *Physics of Plasmas*, **23**, Article ID: 056304. https://doi.org/10.1063/1.4946017

[15] Huntington, C.M., Fiuza, F., Ross, J.S., Zylstra, A.B., Drake, R.P., Froula, D.H., *et al.* (2015) Observation of Magnetic Field Generation via the Weibel Instability in Interpenetrating Plasma Flows. *Nature Physics*, **11**, 173-176. https://doi.org/10.1038/nphys3178

[16] Obergaulinger, M., Janka, H.T. and Aloy, M.A. (2014) Magnetic Field Amplification and Magnetically Supported Explosions of Collapsing, Non-Rotating Stellar Cores. *Monthly Notices of the Royal Astronomical Society*, **445**, 3169-3199. https://doi.org/10.1093/mnras/stu1969

[17] Eilers, A., Hogg, D.W., Rix, H. and Ness, M.K. (2019) The Circular Velocity Curve of the Milky Way from 5 to 25 kpc. *The Astrophysical Journal*, **871**, Article 120. https://doi.org/10.3847/1538-4357/aaf648